LANE 2012

Short-pulse laser processing of CFRP

Rudolf Weber[a,*], Christian Freitag[a,b], Taras V. Kononenko[c], Margit Hafner[a], Volkher Onuseit[a], Peter Berger[a], Thomas Graf[a]

[a]Universität Stuttgart, Institut für Strahlwerkzeuge (IFSW), Pfaffenwaldring 43, D-70569 Stuttgart, Germany
[b]GSaME Graduate School of Excellence advanced Manufacturing Engineering, Nobelstraße 12, 70569 Stuttgart, Germany
[c]General Physics Insitute, Moscow, Russia

- Invited Paper -

Abstract

Short-pulse lasers allow processing of carbon fiber reinforced plastics (CFRP) with very high quality, i.e. showing thermal damage in the range of only a few micrometers. Due to the usually high intensities and the short interaction times of such short pulses, only a small fraction of the incident laser energy is converted to residual heat which does not contribute to the ablation process. However, if the next pulse arrives before the material had time to cool down, i.e. this residual thermal energy did not sufficiently flow out of the interaction region, it encounters material which is still hot. This remaining energy and temperature is summing up during the sequence of pulses and is commonly referred to as "heat accumulation". Thermal damage in addition to the damage created by the process itself is induced, if the resulting temperature sum exceeds the damage temperatures of either the fibre or the plastic.
The current paper presents the influence of the laser parameters such as pulse energy and repetition rate on this heat accumulation. An analytical model was used to describe the heat accumulation for different laser parameters. It describes the heat accumulation process and allows estimating the maximum number of pulses allowed at the same place before a detrimental temperature increase occurs.

Keywords: CFRP; carbon fibre; thermal damage; percussion drilling; heat accumulation

* Corresponding author. Tel.: +49-711-685-66844 ; fax: +49-711-685-66842 .
E-mail address: weber@ifsw.uni-stuttgart.de .

1. Introduction

Carbon fibre reinforced plastic (CFRP) belong to the key materials for future lightweight constructions in automotive and aircraft applications. Actually, even basic tasks such as cutting or drilling require extensive research to be adapted to the unique properties of CFRP. Laser processing is very promising and well established but the very inhomogeneous thermo-physical properties of CFRP make it a challenging task. The properties are summarized in Table 1.

Table 1. Thermo-physical data of CFRP used for model calculations

	Matrix	Carbon fibre parallel/perpendicular to fibre axis
Density ρ in kg/m3	1250	1850
Heat conductivity k in W/m.K	0.2	50/5
Heat capacity c_p in J/kgK	1200	710
Evaporation temperature T_v in K	800	3900
Latent heat L_v in kJ/kg	1000	43000

The main issue is the heat load which can cause large matrix damage. This heat load results from the part of the absorbed laser energy which does not contribute to the ablation process. A minimum thermal damage of the fibre and especially of the matrix can principally not be avoided: During the interaction, a small but not negligible amount of absorbed laser energy is lost into the material through heat conduction. This minimum loss is determined by the intensity of the incident laser light which defines the time necessary to evaporate the volume defined by the optical penetration depth, thermal diffusion length and the beam cross-sectional area. The resulting minimum thermal damage is shown in Fig. 1. [1]. The red and the blue dotted line represent this minimum extent of the evaporation and thermal damage of the matrix material, respectively.
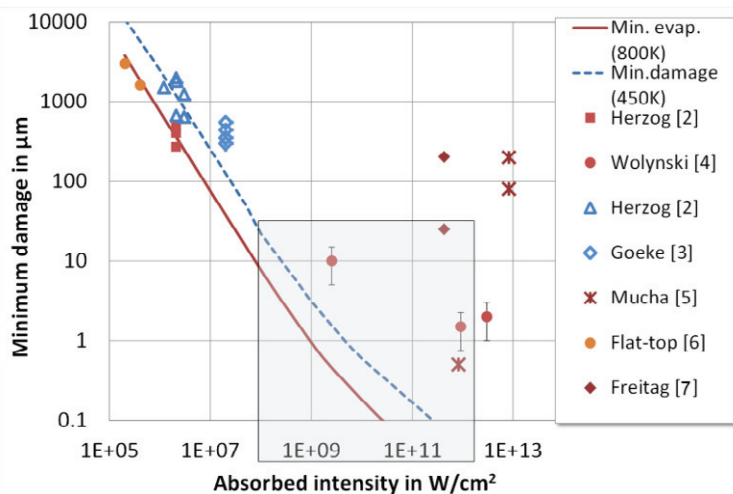

Fig. 1. Minimum possible thermal damage resulting from the process itself as a function of the incident intensity. The shaded area depicts the intensity range of "optimum processing". Lines: theoretical model, points: experimental data

However, when the intensity is increased above values of about 10^{12} W/cm^2 additional effects can cause large matrix damage as shown by the experimental values [2]-[7] in Fig. 1. The shaded area between 10^8 W/cm^2 and 10^{12} W/cm^2 therefore gives an intensity range, where optimum laser processing can be achieved.

Today, intensities above about 10^9 W/cm^2 are only obtained with pulsed lasers using production-relevant focusing conditions (i.e. with f/# larger than about 5). With pulsed lasers, not only the intensity of a single pulse but also the average power defined by the pulse energy and the repetition rate have to be considered: If the repetition rate is too high for the material to cool down between the pulses the heat accumulation leads to thermal damage in addition to the damage created by the process itself, if the resulting temperature exceeds the damage temperatures of either the fibre or the plastic.

2. Heat accumulation model

Several approaches for numerical and empirical simulation of the thermal damage in CFRP are summarized in Ref. [8]. However, analytical models are well suited to analyze and understand the basic physical mechanisms of the laser material interaction. "Heat accumulation" is defined in this paper as the "residual temperature before arrival of the subsequent pulse". In short-pulse laser processing the time during which the energy is applied to the material is much shorter than the time between two subsequent pulses (typically more than 1000x for ps- and ns-lasers). Therefore, the solutions of the heat conduction equation presented in [9] are very well suited to describe the temporal evolution of the temperature distribution inside the processed material. In view of the material structure of CFRP which is strongly organized in layers the 2-dimensional solution is considered to be appropriate. Convective and radiative losses can be neglected in our geometry. The temperature increase caused by the absorbed energy per unit length $Q_{\ell,Therm}$ then reads:

$$\Delta T_{2D} = \frac{Q_{\ell,Therm}}{\rho \cdot c_p \cdot 4 \cdot \pi \cdot \kappa \cdot t} \cdot e^{-\frac{r^2}{4 \cdot \kappa \cdot t}} \qquad \text{with} \qquad r^2 = x^2 + y^2 \qquad (1)$$

where ρ is the material density, c_p is the heat capacity and $\kappa = k/\rho\,c_p$ the thermal diffusivity with k being the thermal conductivity. Eq. (1) describes the temporal and spatial evolution of the temperature increase caused by absorbed energy which is converted to heat and does not contribute to the ablation process. The energy per unit length $Q_{\ell,Therm}$ is applied instantaneously, i.e. eq. (1) only describes the cooling phase. It is valid for times which are "much longer" than the duration of the energy input which suits well to our situation of short-pulse lasers as stated above.

An important value for the calculation is the amount of the heating energy per unit length, $Q_{\ell,Therm}$ which is given by:

$$Q_{\ell,Therm} = \frac{\eta_{L,Therm} \cdot \eta_{Abs} \cdot E_{Pulse}}{z_{Interaction}} \qquad (2)$$

where E_{Pulse} is the incident pulse energy, η_{Abs} is the absorptivity, determining the fraction of light converted to heat energy, and $\eta_{L,Therm}$ is the fraction of the heat energy which does not contribute to the ablation process and hence is left in the material.

As discussed for example in Ref. [10] and [11] both, the pulse energy itself and the spatial profile of the pulse have a significant influence on the amount of absorbed heat energy and therefore also influence the overall process efficiency. For the current paper the fraction of heat energy left in the material was assumed to be constant with a value of $\eta_{Abs} \cdot \eta_{L,Therm} = 8\%$. This is believed to hold for the parameters applied in the current experiments as they were all performed at the same pulse energy of 28 µJ and the same focus diameter of 33 µm. For the calculations it is furthermore assumed that the laser pulses are absorbed at the bottom of the groove (or borehole) along a distance in the beam propagation direction, $z_{Interaction}$, of one focus radius, i.e. $z_{Interaction} = 16.5$ µm. This corresponds to about 2 to 3 layers of carbon fibres.

From geometrical considerations and in view of the 1-D and 3-D solutions in Ref [9] it can readily be assumed that the significantly different thermal diffusivities in x- and y-directions can be accounted for by modifying eq. (1) to eq. (1a):

$$\Delta T_{2D} = \frac{Q_{\ell,Therm}}{\rho \cdot c_p \cdot 4 \cdot \pi \cdot \sqrt{\kappa_x}\sqrt{\kappa_y} \cdot t} \cdot e^{-\frac{1}{4 \cdot t}\left(\frac{x^2}{\kappa_x}+\frac{y^2}{\kappa_y}\right)} \tag{1a}$$

Equations (1) and (1a) describe the evolution of the temperature increase caused by one single pulse. In order to calculate a series of pulses, the following modification of eq. (1a) is applied to describe the temperature evolution caused by the nth pulse:

$$\Delta T_{2D} = \Phi\left(t - \frac{n}{f}\right) \cdot \frac{Q_{\ell,Therm}}{\rho \cdot c_p \cdot 4 \cdot \pi \cdot \left(t - \frac{n}{f}\right)\sqrt{\kappa_x}\sqrt{\kappa_y}} \cdot e^{-\frac{1}{4\left(t-\frac{n}{f}\right)}\left(\frac{x^2}{\kappa_x}+\frac{y^2}{\kappa_y}\right)} \tag{3}$$

The Heaviside function is $\Phi(A) = 0$ for an argument $A < 0$ and $\Phi(A) = 1$ for $A \geq 0$.

For temperature independent material parameters, the resulting temperature distribution is then simply found be the sum

$$\Delta T_{Sum} = \sum_{n=1}^{N_{Pulses}} \Delta T_{2D} \tag{4}$$

where N_{Pulses} is the total number of considered laser pulses.

As an example the resulting sum at the location of the energy input (x = y = 0 mm) is shown in Fig. 2 for the material parameters given in Table 1and an input heat of $Q_{\ell,Therm} = 0.22$ J/m for repetition rates of 800 kHz (dark red) and 80 kHz (dark green). After 35 µs the heating (laser) is switched off and the surface cools down. The bright red dashed line indicates a temperature increase by 500 K above ambient temperature (300 K) which corresponds to the matrix evaporation temperature of 800 K.
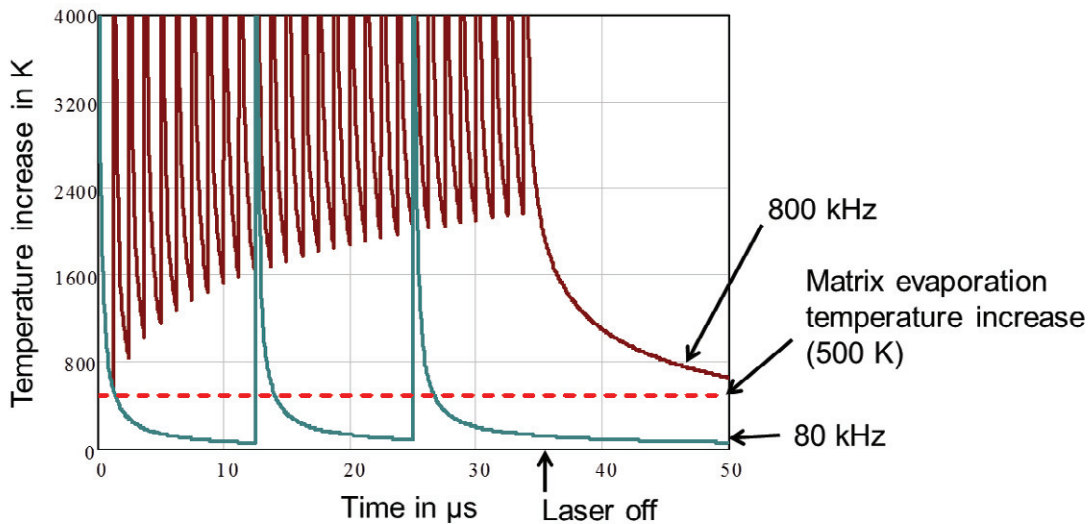
Fig. 2. Calculated "Heat accumulation" caused by subsequent pulses for different frequencies

It can clearly be seen that the processing at high frequency (dark red line) suffers from a high residual temperature after each pulse which is continuously summing up. On the other hand, with the low frequency (dark green line) the material has time to almost completely cool down between the pulses. In addition it is seen that with 800 kHz already at the second pulse the surface is still hotter than the matrix evaporation temperature. Therefore, strong matrix damage is expected at 800 kHz while with 80 kHz much less damage should occur. After a strong increase of the accumulation temperature in the first 20 µs the curve with 800-kHz shows a saturation-like behavior.

The evolution of the temperature at the origin of the energy input gives a good insight into the process of heat accumulation. However, the value of interest is the extent of the matrix evaporation zone (MEZ). In the following it is assumed that the MEZ is given by the distance of the 800 K isotherm from the interaction zone. Eq. 4 was solved numerically to calculate the reach of the 800 K isotherm. Fig. 3 shows the reach of the 800 K isotherm along the fibres as a function of time, calculated as an example for an absorbed energy per unit length of 0.08 J/m and a frequency of 800 kHz.
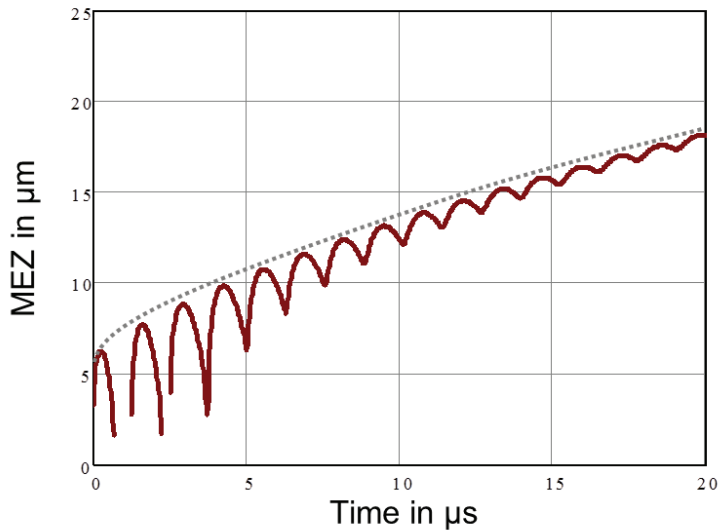
Fig. 3.   MEZ (i.e. reach of the 800 K isotherm) for the first 16 pulses at 800 kHz and 0.08 J/m. The grey dotted line is the envelope of the isotherm reach giving the actual extent of the correspondingly evaporating matrix material

For the first few pulses at the beginning of the pulse sequence it is seen, that the location of the 800 K isotherm reaches a clear maximum for each pulse and then propagated back to almost zero. When the number of pulses increases, the remaining heat in the material also increases and the temporary maximum of the reach gets less and less pronounced. This means that if heat accumulation can build up the damage is more and more determined by the average power than by the single pulse energy. It is important to note that the visible matrix evaporation zone is given by the envelope of this curve which is represented by the grey dotted line.

Very often, maximum allowed material damage is specified due to the requirements of an application. With this calculation it is possible to determine the maximum number of pulses at a given repetition rate which are allowed at a single position to meet such specifications.

3. Experiments

The experiments were performed with a TruMicro 5250 ps-laser at a wavelength of 515 nm, an M^2 of 1.3, a pulse duration of 8 ps, a maximum average power on target of 23 W, and at a repetition rate of 800 kHz. The beam was focused onto the CFRP surface in a spot of 33 μm in diameter. The process region was illuminated with an 800-nm diode laser and observed with a high-speed camera. Biaxial CFRP with a thermoset matrix material was processed with different laser parameters in order to investigate the influence of heat accumulation. High speed records for two different parameter sets at the same pulse energy of 28 μJ were made: *Set 1* with 80 kHz at a feed rate of 10 m/min and *Set 2* with 800 kHz at a feed rate of 2 m/min. The resulting surface seen while processing is shown in Fig. 4(a) for *Set 1* and in Fig. 4(b) for *Set 2*. The matrix evaporation zone with the low repetition rate in Fig. 4(a) is asymmetric, 25 μm on the left side and 10 μm on the right side of the kerf. At the high repetition rate seen in Fig. 4(b) the evaporation zone has an average extent of about 225 μm.
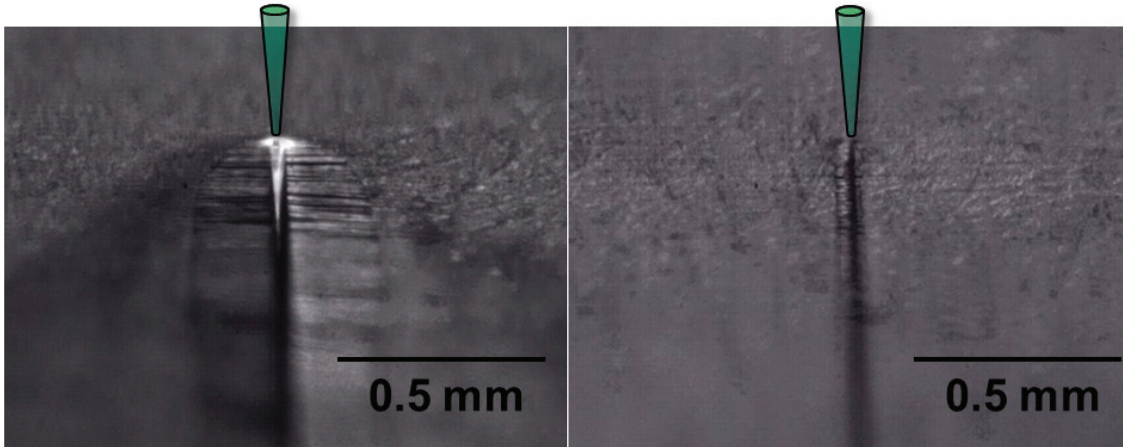
Fig. 4.   High speed records of the CFRP surface processed with: (a) 28 μJ, 10 m/min, 80 kHz, t_{int} = 0.2 ms, MEZ = 25 μm; (b) 28 μJ, 2 m/min, 800 kHz, t_{int} = 1.0 ms, MEZ = 225 μm

The interaction time t_{int} defines how long thermal loss energy is applied to a given point in the material. It is given by the focal spot diameter divided by the feed rate. In the calculations, the heating is switched off after this interaction time. For the two parameters described above the interaction time is t_{int} = 0.2 ms in Fig. 4(a) and t_{int} = 1.0 ms in Fig. 4(b).

The extent of the matrix evaporation zone was calculated with the heat accumulation model as described above and for the parameters in Fig. 4 and Table 1. The extent of the damage seen in Fig. 4(b) was used to calibrate the fraction of absorbed thermal energy (as mentioned above, $\eta_{Abs} \cdot \eta_{L,Therm}$ = 8%). The results of the calculation are shown in Fig. 5, the blue line for *Set 1* and the red line for *Set 2*. The black arrows denote the respective end of the interaction time. The inset is a magnification of the first 250μs showing that only weak heat accumulation occurs at the low repetition rate in connection with the high feed rate.
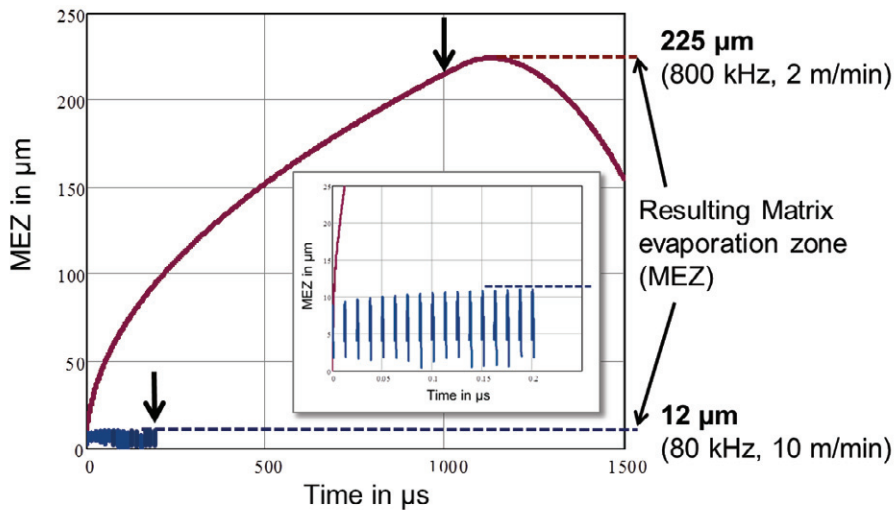

Fig. 5.   Calculated matrix evaporation ZONE for 800 kHz, 2 m/min (red) and 80 kHz, 10 m/min (blue)

The red line shows that the isotherm continues to expand further for about 200 µs after the end of the interaction time, i.e. after the laser has passed the interaction region. This behavior can also be noticed in Fig. 4(b). The dotted line marks the largest extent of the matrix evaporation zone. The 80 kHz result was calculated with the same 8% of absorbed fraction as described above showing a reasonable agreement with the experimental value.

In a second experiment, the line energy input along the feed direction was held constant at 112 J/m for two different parameter sets: *Set 3* with 8 kHz and a feed rate of 0.12 m/min and *Set 4* with 800 kHz and a feed rate of 12 m/min, both with a pulse energy of 28 µJ. Fig. 6 shows the cross-sections which were made from these cuts. The green cone at the top marks the location of the laser. The top dark grey layer is the matrix material which covers the fibres. The bright layers are fibres with orientation parallel to the picture surface; the grey-brown layers are fibres with orientation perpendicular to the picture surface. The cross-sections clearly demonstrate the effect of heat accumulation. While nearly no damage can be observed with *Set 3* in Fig. 6(a), significant matrix damage is created with *Set 2* shown in Fig. 6(b). It can be seen that different extents of the damage occur, as marked in the picture.

Only about 30 µm of damage is noticeable at the beam entrance. This is believed to result from the relatively thick matrix layer on the top. On the top of the parallel layer, the damage of the matrix expands to 125 µm. This is what usually would be seen with a thin surface matrix layer as seen in Fig. 6(a). This means that the assumption that the 800 K isotherm represents the matrix evaporation region is only valid in the vicinity of the fibers. If the matrix layer is thicker than a few ten micrometers, both, the energy required for matrix evaporation and the thermal conductivity inside the matrix material would have to be considered in addition.

Inside the parallel layer the damage extends to 165 µm. The dark region is a result from cracking of the fibres during the grinding process and indicates the region where the matrix is destroyed.

Further below, the perpendicular layer suffers from a damage of about 65 µm. It is noted that at the interface between parallel and perpendicular orientation almost no vertical heat flow can be observed confirming the assumption of a 2-D heat flow.
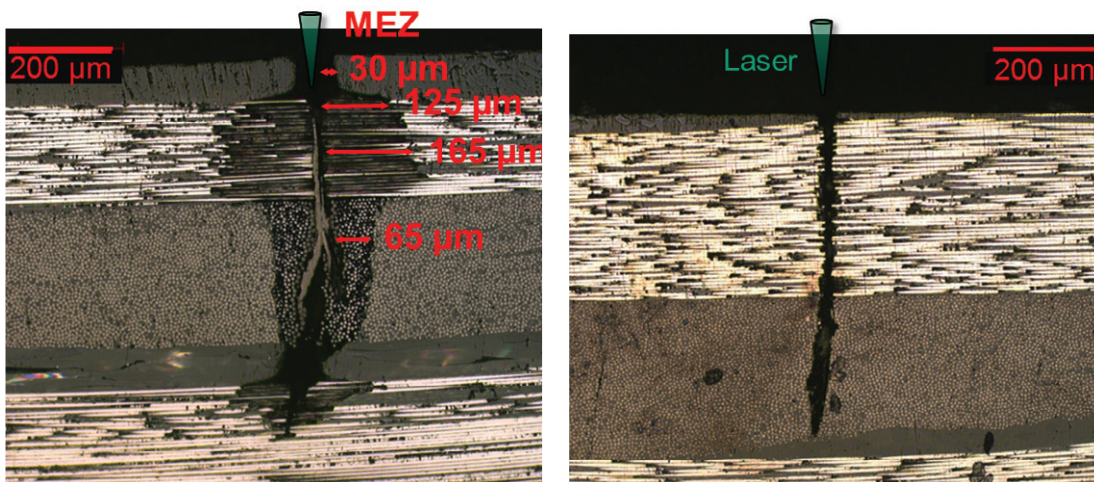

Fig. 6.   Cross-sections of CFRP processed with: (a) 28 µJ, 0.12 m/min, 8 kHz, t_{int} = 16.7 ms; (b) 28 µJ, 12 m/min, 800 kHz, t_{int} = 0.167 ms

As shown in Fig. 7 the observed extent of the damage is again confirmed by the result of the calculation, again using the same fraction of 8% for the absorbed thermal energy left in the material. The blue curve calculated for *Set 3* (details shown in the inset) clearly shows that no heat accumulation occurs with 8 kHz and 28 µJ and hence the interaction region can completely cool down between the pulses. Therefore the maximum extent of the matrix evaporation zone is determined by the extent of about 8 µm resulting from each single pulse a seen in the inset.
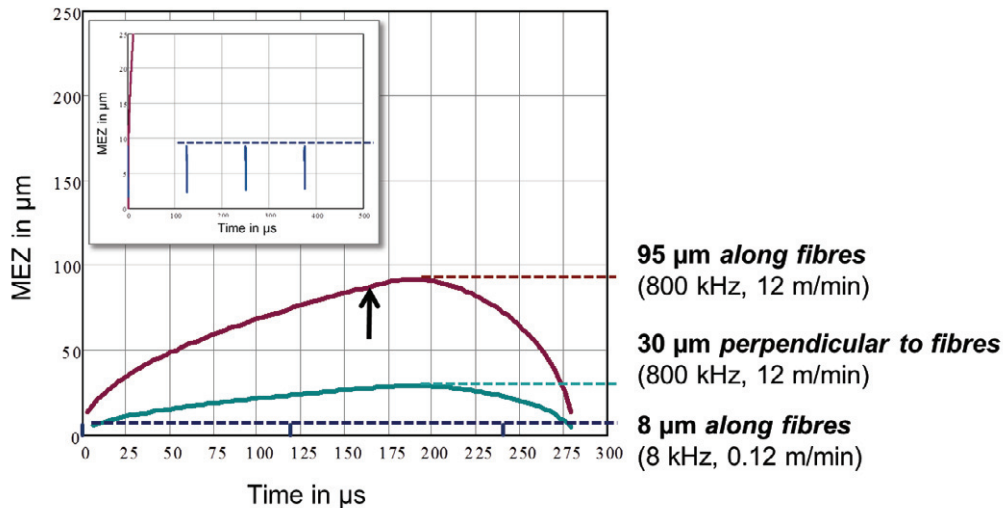

Fig. 7.   Calculated extent of the 500 K isotherm for 800 kHz, 12 m/min (red) and 8 kHz, 0.12 m/min (blue)

The red curve shows the extent of the matrix evaporation zone along the direction of the fibers for *Set 4*; the green line the one perpendicular to the fibers. The maximum extent in the direction of the fibers is about 95 µm and about 30 µm perpendicular to the fibers, as indicated by the two dashed lines. The ratio of the two extents is 3.2. It is noted that this is calculated with the transversal and longitudinal heat conductivities given in Table 1 with a ratio of 10. The ratio of the measured extent of the matrix evaporation zone in Fig. 6(b) is 165 µm/65µm = 2.5 which would require a ratio of the heat conductivities of 6.3 in the calculations (e.g. increasing $k_{perpendicular}$ from 5 W/mK to 8 W/mK). This slight modification of the material parameters is very reasonable regarding the complexity of CFRP.

Although the extent of 95µm calculated in the direction of the fibres (red line) agree fairly well with the about measured 125 to 165µm in Fig. 6(b) the large fluctuation of the extents of the matrix damage proves that the definition of a "damage extent" as well as a firm calibration of the model need much more additional work.

Not within the scope of this paper but nevertheless interesting further features are seen in Fig. 6(b): The kerf bends towards the left in the bottom region and widens. In addition there is some (not yet identified) debris inside the kerf which does not originate from the grinding process.

4. Conclusion

An analytical model was presented which allows calculating heat accumulation effects in pulsed laser processing of CFRP. The model accurately predicts the thermal damage which can be expected from different laser and machine parameters.

The findings have strong impact on the design of laser systems for CFRP processing. It can be concluded that high repetition rates require special efforts to prevent matrix damage caused by heat accumulation, i.e. the interaction time has to be very short in order to have only a few subsequent pulses in the interaction region. This means that with high-frequency short-pulse lasers very high feed rates are required. Especially remote processing systems as presented for cw lasers in Ref. [12] are promising due to their fast beam movement capabilities. However, short-pulse lasers with average powers well above 1 kW needed for industry-relevant productivity will demand a new generation of laser processing systems [13]. This makes tools as presented in this paper very useful which allow determining mandatory performance boundaries for layout and design of such systems.

Acknowledgement

References

[1]   R. Weber, M. Hafner, A. Michalowksi, T. Graf; Minimum damage in CFRP laser processing, Physics Proceedia 12(2), 2011, Pages 302-310.

[2]   D. Herzog, P. Jaeschke, O. Meier and H. Haferkamp, Investigations on the thermal effect caused by laser cutting with respect to static strength of CFRP, International Journal of Machine Tools & Manufacture 48 (2008), pp. 1464–1473.

[3]   A. Goeke and C. Emmelmann, Influence of Laser Cutting Parameters on CFRP Part Quality, Physics Proceedia 5 (2010), pp. 253–258.

[4]   A. Wolynski, H. Haloui, P. Mucha, A. Gleite, P. French, R. Weber, T. Graf; Effect of process strategies on thermal load during CFRP processing, Proc. ICALEO 2010, Los Angeles.

[5]   P. Mucha; Experimentelle Untersuchungen zur Laserbearbeitung von CFK mit Pikosekundenpulsen bei 532 nm, Studienarbeit IFSW 10-37 (2010).

[6]   R. Weber, M. Hafner, A. Michalowski, P. Mucha, T. Graf; Analysis of thermal damage in laser processing of CFRP, Proc. ICALEO 2011.

[7]   C. Freitag, M. Hafner, A. Michalowski, V. Onuseit, R. Weber, P. Berger, T. Graf; Diagnostics of basic effects in laser processing of CFRP, LPCC 2012.

[8]   A.A. Cenna, P. Mathew; Evaluation of cut quality of fibre-reinforced plastic – a review; Int. J. Mach. Tools Manufact., Vol. 37 (6), 723-736 (1997).

[9]   N.N. Rykalin; Die Wärmegrundlagen des Schweißvorgangs. VEB Verlag Technik, Berlin, 1957
      D. Radaj; Heat Effects of Welding, Temperature Field, Residual Stress, Distortion; Springer Verlag Berlin Heidelberg (ISBN 3-540-54820-3), 1992.

[10] B. Neuenschwander, B. Jäggi, M. Schmid; Factors controlling the ablation efficiency for ultra-short pulses between 250fs and 50ps, SLT12, , Neue Messe Stuttgart, 2012.

[11] M. Hafner, R. Weber, T. Graf; Modeling of laser ablation of CFRP – influence of beam profile, Stuttgarter Lasertage SLT 12, Neue Messe Stuttgart, 2012.

[12] A. Klotzbach, M. Hauser, E. Beyer; Laser Cutting of Carbon Fiber Reinforced Polymers using Highly Brilliant Laser Beam Sources, Physics Procedia, 12, Part A, 572–577, 2011.

[13] T. Graf, R. Weber, V. Onuseit, M. Hafner, C. Freitag, A. Feuer; Laser Applications from Production to Machining of Composite Materials, EALA 2012.